A GaN-Based Insulated-Gate Photoconductive Semiconductor Switch for Ultrashort High-Power Electric Pulses

Xinmei Wang, *Member, IEEE*, Sudip K. Mazumder, *Senior Member, IEEE*, and Wei Shi

***Abstract*— For monolithic realization of a traditional photoconductive semiconductor switch (PCSS) incorporating a high-voltage pulsed bias, an insulated-gate photoconductive semiconductor switch (IGPCSS) structure is proposed. The insulated-gate cells in this structure can aid the laser-triggered area to dynamically obtain a much higher bias voltage than the dc withstand voltage of a traditional PCSS. The static and the dynamic characteristics of a GaN-based IGPCSS triggered by a subbandgap laser are analyzed, and the results show that its photoelectric-conversion efficiency is twice that of a dc-charged traditional GaN-based PCSS for same triggering conditions.**

***Index Terms*— Photoconductive switch, pulsed power, MISFET, GaN.**

I. Introduction

A PHOTOCONDUCTIVE semiconductor switch triggered with an ultra-short pulsed laser is a type of low-jitter ultra-broadband high-power device without potential spurious triggering caused by electro-magnetic interference (EMI) [1], [2]. To avoid the use of expensive ultraviolet laser, the wide-band-gap PCSS is usually made of highly-compensated semi-insulating material with sub-bandgap absorption ability, such as GaN:Fe [3] or SiC:V [4]. However, its dark-state current characteristic is remarkably nonlinear, which is mainly caused by the unavoidable high-concentration deep energy levels. It is known that, a high-voltage pulsed source, such as a Marx circuit [5], can significantly improve the device lifetime and the photoelectric response [6], but it also leads to higher cost and problem with portability, especially when high repetition rate is required.

Therefore, it is necessary to design a novel PCSS with an electric power switch structure vertically integrated to share the dc-bias voltage. Considering that the repetition rate of a traditional PCSS can reach up to hundreds of megahertz, the structure of multi-cell U-shape n-channel MISFET is the best selection to the design of the novel PCSS. In this letter, the design principles are presented, the voltage and the current formulas are deduced, and the expected effect is validated through the simulation of a relevant GaN-based device sample.

Manuscript received February 18, 2015; revised March 13, 2015; accepted March 14, 2015. Date of publication March 24, 2015. This work was supported in part by the National Natural Science Foundation of China under Grant 60906029 and in part by the University of Illinois at Chicago, Chicago, IL, USA. The review of this letter was arranged by Editor T. Egawa.

X. Wang is with the Xi'an University of Technology, Xi'an 710048, China. She is now a visiting scholar at the University of Illinois at Chicago, Chicago, IL 60607 USA.

S. K. Mazumder is with the University of Illinois at Chicago, Chicago, IL 60607 USA (e-mail: mazumder@uic.edu).

W. Shi is with the Xi'an University of Technology, Xi'an 710048, China.

Color versions of one or more of the figures in this letter are available online at http://ieeexplore.ieee.org.

Digital Object Identifier 10.1109/LED.2015.2416188

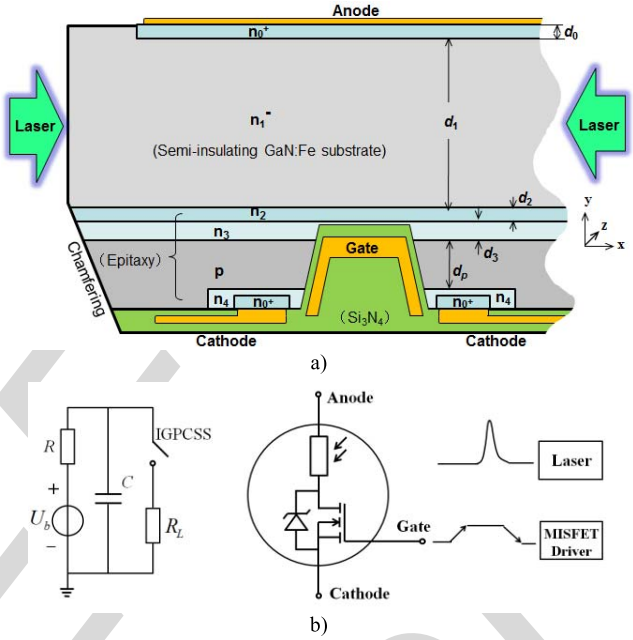

Fig. 1. a) Lateral view of the GaN-based IGPCSS. b) Equivalent circuit model of the IGPCSS device (middle), illustrating the schematic diagrams of a bias source (left) and the timing sequence of trigger signals (right).

II. Design

A. IGPCSS Structure and Triggering Method

The insulated-gate PCSS structure is illustrated in Figs. 1a and 2. The U-shaped MISFET cells are fabricated in the GaN epitaxy layers which grow on a semi-insulating GaN:Fe substrate. The unintentionally-introduced shallow donor levels in the GaN substrate result from the O on N-sites, Si on Ga-sites and N-vacancies [7], [8]. The iron impurities, as deep acceptor sources, are intentionally heavy doped ($\sim 10^{18}$ cm^{-3}) to compensate the shallow donors for making the substrate dark resistivity up to $1 \times 10^9 \Omega \cdot$cm, and meanwhile the substrate carrier lifetime sharply decreases to $<$ 1ns [3]. A gate-voltage pulse makes the channel entirely open and then two rows of 1-ns-pulsewidth 1-mJ-energy 532-nm-wavelength laser beams simultaneously illuminate the semi-insulating substrate from opposing sides. The equivalent circuit model composes of a traditional PCSS, an n-channel normally-closed MISFET, and a voltage-stabilizing diode, as illustrated in Fig. 1b.

A few of methods are used to increase the safe operating area of the IGPCSS. The laser fibers are grouped into two rows, and the directions of the laser beams are interdigitated each other (see Fig. 2) to prevent the current crowding happened in the laser-triggered area. The multi-cell parallel connection and the light-doping transition (see n_3 and

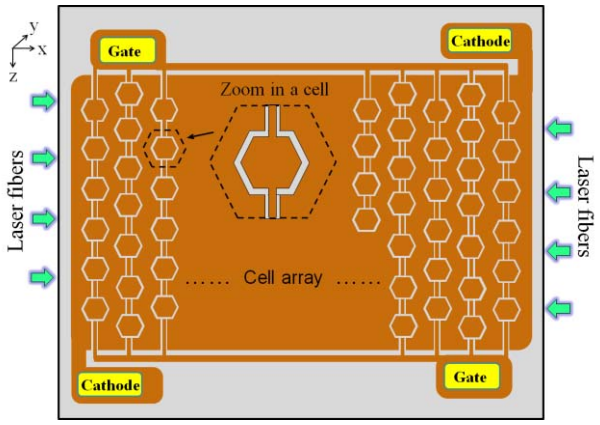

Fig. 2. Bottom view (upper half) of the GaN-based IGPCSS.

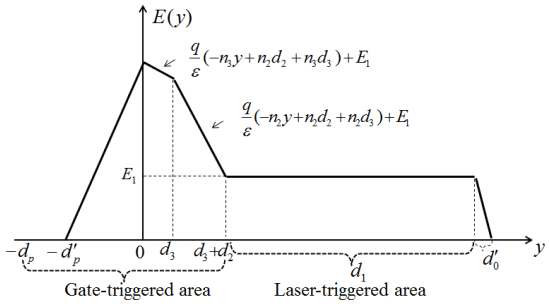

Fig. 3. Electric-field distribution of the IGPCSS under dark-state condition and a dc-bias voltage.

n_4 layers) for the n-channels terminals are designed to prevent the current crowding enhenced in the gate-triggered area. Furthermore, the chamfer processes is helpful to improve the blocking voltage ability of the gate-triggered area.

B. Static Voltage Distribution

The static distribution of the electric field across the IGPCSS before it is triggered by an electrical gate signal is shown in Fig. 3. The space charges in the n_1 layer can be ignored due to the semi-insulating property, and hence the electric field across the n_1 layer in the y direction (E_1) is regarded as a constant. The voltage drop due to the bulk resistances of the n_4, p, n_0 layers can be ignored, since their conductivities are much higher than that of the semi-insulating substrate. Moreover, the voltage drop across the positively biased p-n_4 junction can be ignored when the IGPCSS is biased with high voltage. Therefore, through integrating the electric field curve of Fig. 3, the static voltage across the gate-triggered area is given by

$$V_{th} = k\left[\frac{q}{\varepsilon}\left(\frac{pd_p'^2}{2}+\frac{n_3d_3^2}{2}+n_2d_2d_3+\frac{n_2d_2^2}{2}\right)+E_1(d_2+d_3)\right],$$
$$E_1=\frac{U_b-V_{th}}{d_1},\quad d_p'=\frac{n_2d_2+n_3d_3+\frac{\varepsilon E_1}{q}}{p}. \quad (1)$$

In (1), q is the elementary charge, ε is the dielectric constant of the epitaxial material, and k (<1) is a semi-empirical coefficient which is used to linearly simplify the effect caused by the x-directed extension of the carrier-depleted region along the insulated gate. It is noted that, the thickness of the p-type epitaxy layer (d_p in the Fig. 1) should be more than the minimum design value (d_p'), or the pn junction will be punched through undesirably from the cathode side. Equation (1) yields that V_{th} will monotonically slightly change following the bias voltage and the substrate thickness, as shown in Fig. 4.

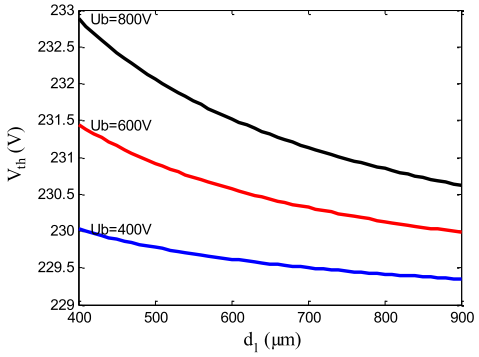

Fig. 4. Variation of the static voltage across the gate-triggered area of the IGPCSS under dark-state condition for varying the dc-bias voltages (U_b) and the substrate thickness (d_1). The curves are calculated based on (1) where $d_2 = 1.5$ μm, $d_3 = 0.5$ μm, $k = 0.25$ and n_2, n_3 and p are 5×10^{16}, 1×10^{15}, and 8×10^{15} cm^{-3}, respectively.

C. Photocurrent Distribution

To design the relevant heat-dissipation accessory of the IGPCSS, the photocurrent distribution in the x direction is estimated roughly. The density of the gallium-site Fe^{3+} deep energy level is much higher than those of any other energy levels in the GaN:Fe [8]. It means that the two-step photon absorption from valence band to conduction band via the Fe^{3+} levels is dominant, if the laser wavelength is less than 585 nm (i.e., 3.42 eV-1.299 eV [8]). Therefore, the optical intensity distribution in the IGPCSS can be given by

$$I(x,t)=I_0[e^{-\alpha_{eff}x}+e^{-\alpha_{eff}(L-x)}]G(t). \quad (2)$$

In (2), I_0 is the initial optical intensity of the incident laser only from one side of the IGPCSS, G is a Gaussian function, and α_{eff} is the effective absorption coefficient to linearly simplify the two-step photon absorption via the high-density deep energy levels [3]. Considering that the cost of the power pulsed laser device is typically incorporated in the total cost of the switch system, the lost laser energy transmitted from the opposite sides of the IGPCSS is expected to be less than 5% of the incident energy. The x-directed device length (L) can be roughly estimated based on (2).

The rate for the photon-generated electrons (n) in the semi-insulating GaN substrate is given by

$$\frac{\partial n(x,t)}{\partial t}=-\frac{1}{2\hbar\omega}\frac{\partial I(x,t)}{\partial x}-\frac{n(x,t)}{\tau_r} \quad (3)$$

where $\hbar\omega$ is the photon energy and τ_r is the effective recombination rate. Therefore, the peak electron density is deduced by setting $\frac{\partial n(x,t)}{\partial t}=0$ to obtain the following:

$$n\left(x,t_{peak}\right)=\frac{\tau_r\alpha_{eff}}{2\hbar\omega}I\left(x,t_{peak}\right) \quad (4)$$

where $I\left(x,t_{peak}\right)$ is obtained using (2). The peak conductivity is given by

$$\sigma(x,t_{peak})=qn(x,t_{peak})(\mu_n+\mu_p) \quad (5)$$

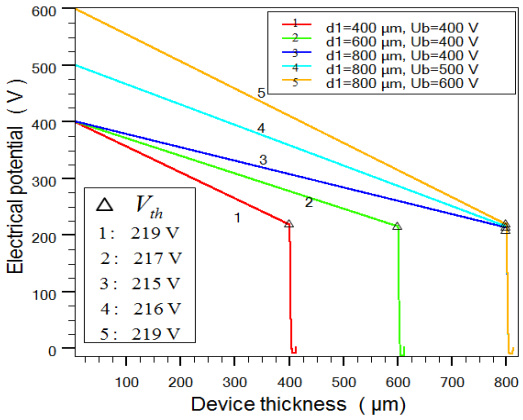

Fig. 5. Static voltage distribution in the y direction, simulated when $d_0 = 0.5$ μm, $d_2 = 1.5$ μm, $d_3 = 0.5$ μm, $d_p = 10$ μm, and n_0, n_1, n_2, n_3, n_4 and p are 8×10^{19}, 6.2×10^6, 5×10^{16}, 1×10^{15}, 1×10^{17} and 8×10^{15} cm^{-3}, respectively.

where μ_n and μ_p are the electron and the hole mobilities, respectively. The current density is proportional to the conductivity, which results in

$$J\left(x, t_{peak}\right) \propto [e^{-\alpha_{eff} x} + e^{-\alpha_{eff}(L-x)}]. \quad (6)$$

III. Analysis and Comparison

The static voltage distributions are simulated using Silvaco [9] and the results are shown in Fig. 5. The voltage across the gate-triggered area slightly decreases with d_1 and slightly increases with U_b. These variations are in agreement with the above conclusions calculated based on (1). It is noted that, the voltage across the gate-triggered area is approximatively a constant, which validates the equivalent circuit model of the IGPCSS in Fig. 1b. Therefore, there exist two thresholds for the IGPCSS device to output photocurrents: one, which represents the gate voltage when the n-channels are just formed; and the other, which represents the bias voltage when the p-n junction is just punched through.

Next, the leakage current and the transient characteristics of an IGPCSS with a punch-through voltage of 400 V are simulated. The simulation model and the results are shown in Fig. 6. With the IGPCSS being electrically triggered by the gate, the voltage across the gate-triggered area is gradually transferred to the laser-triggered area (see the orange curve in Fig. 6c), which enhances the electric field across the IGPCSS laser-triggered area from 6.7 kV/cm to 13.4 kV/cm.

Third, a comparable traditional PCSS (CT-PCSS) model (see Fig. 6b) are simulated, which have the same material, size, ohmic electrodes, static electric field and laser as that of the IGPCSS. The result demonstrates that the leakage current of the IGPCSS is far less than that of the CT-PCSS owing to the p-n junction. Furthermore, the results demonstrate that the IGPCSS yields higher photocurrent peaks than the CT-PCSS. The photoelectric-conversion efficiency of the IGPCSS (η_{IG}) is higher than that of the CT-PCSS (η_{CT}). The photoelectric-conversion efficiency is referred in this letter as the ratio of the output photocurrent peak and the relevant input single-pulse laser energy. The efficiency increment ($\eta_{\mathrm{IG}} - \eta_{\mathrm{CT}}$) is approximatively proportional to $U_b/(U_b - V_{th})$ if the enhenced transient electric field across the IGPCSS laser-triggered area is still in the velocity-field linear range (i.e., below 200 kV/cm for the wurtzite GaN material used [10]. Considering V_{th} is almost a constant for varying U_b, it is concluded that, the photoelectric-conversion efficiency of the IGPCSS can be controlled relatively easily by varying the dc-bias voltage.

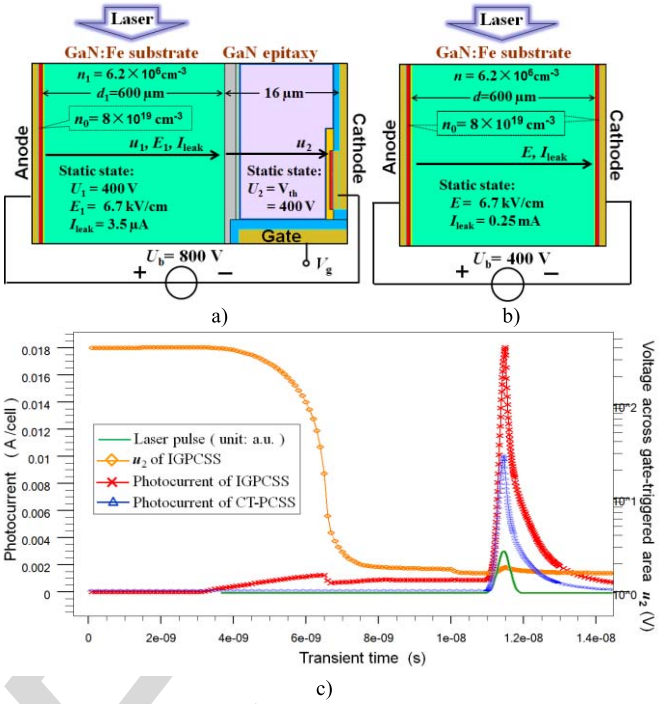

Fig. 6. Characteristics of a) the IGPCSS and b) the CT-PCSS. c) Transient simulation results for the IGPCSS when the gate voltage of the IGPCSS linealy rises from 0 V to 10 V in the first 10 ns and then stays at 10V.

IV. Conclusion

A novel insulated-gate photoconductive semiconductor switch (IGPCSS) structure is presented. It attains a monolithic integration of a PCSS and MISFET cells thereby yielding less leakage current and higher photoelectric-conversion efficiency compared to a relevant traditional PCSS. Through the simulation analyses of the static and the dynamic characteristics, the GaN-based IGPCSS design is validated.

References

[1] P. Kirawanich, S. J. Yakura, and N. E. Islam, "Study of high-power wideband terahertz-pulse generation using integrated high-speed photoconductive semiconductor switches," *IEEE Trans. Plasma Sci.*, vol. 37, no. 1, pp. 219–228, Jan. 2009.

[2] W. Shi and Z. Fu, "2-kV and 1.5-kA semi-insulating GaAs photoconductive semiconductor switch," *IEEE Trans. Electron Device Lett.*, vol. 34, no. 1, pp. 93–95, Jan. 2013.

[3] J. H. Leach *et al.*, "High voltage bulk GaN-based photoconductive switches for pulsed power applications," *Proc. SPIE, Gallium Nitride Mater. Devices VIII*, vol. 8625, pp. 86251Z-1–86251Z-7, Mar. 2013.

[4] J. S. Sullivan and J. R. Stanley, "6H-SiC photoconductive switches triggered at below bandgap wavelengths," *IEEE Trans. Dielectr. Electr. Insul.*, vol. 14, no. 4, pp. 980–985, Aug. 2007.

[5] J.-H. Kim *et al.*, "High voltage Marx generator implementation using IGBT stacks," *IEEE Trans. Dielectr. Electr. Insul.*, vol. 14, no. 4, pp. 931–936, Aug. 2007.

[6] S. F. Glover *et al.*, "Pulsed- and DC-charged PCSS-based trigger generators," *IEEE Trans. Plasma Sci.*, vol. 38, no. 10, pp. 2701–2707, Oct. 2010.

[7] D. O. Dumcenco *et al.*, "Characterization of freestanding semi-insulating Fe-doped GaN by photoluminescence and electromodulation spectroscopy," *J. Appl. Phys.*, vol. 109, no. 12, pp. 123508-1–123508-6, Jun. 2011.

[8] A. Y. Polyakov *et al.*, "Properties of Fe-doped, thick, freestanding GaN crystals grown by hydride vapor phase epitaxy," *J. Vac. Sci. Technol. B*, vol. 25, no. 3, pp. 686–690, 2007.

[9] *Atlas User's Manual*. [Online]. Available: http://www.silvaco.com

[10] S. Chen and G. Wang, "High-field properties of carrier transport in bulk wurtzite GaN: A Monte Carlo perspective," *J. Appl. Phys.*, vol. 103, no. 2, pp. 023703-1–023703-6, Jan. 2008.

A GaN-Based Insulated-Gate Photoconductive Semiconductor Switch for Ultrashort High-Power Electric Pulses

Xinmei Wang, *Member, IEEE*, Sudip K. Mazumder, *Senior Member, IEEE*, and Wei Shi

***Abstract*— For monolithic realization of a traditional photoconductive semiconductor switch (PCSS) incorporating a high-voltage pulsed bias, an insulated-gate photoconductive semiconductor switch (IGPCSS) structure is proposed. The insulated-gate cells in this structure can aid the laser-triggered area to dynamically obtain a much higher bias voltage than the dc withstand voltage of a traditional PCSS. The static and the dynamic characteristics of a GaN-based IGPCSS triggered by a subbandgap laser are analyzed, and the results show that its photoelectric-conversion efficiency is twice that of a dc-charged traditional GaN-based PCSS for same triggering conditions.**

***Index Terms*— Photoconductive switch, pulsed power, MISFET, GaN.**

I. Introduction

A PHOTOCONDUCTIVE semiconductor switch triggered with an ultra-short pulsed laser is a type of low-jitter ultra-broadband high-power device without potential spurious triggering caused by electro-magnetic interference (EMI) [1], [2]. To avoid the use of expensive ultraviolet laser, the wide-band-gap PCSS is usually made of highly-compensated semi-insulating material with sub-bandgap absorption ability, such as GaN:Fe [3] or SiC:V [4]. However, its dark-state current characteristic is remarkably nonlinear, which is mainly caused by the unavoidable high-concentration deep energy levels. It is known that, a high-voltage pulsed source, such as a Marx circuit [5], can significantly improve the device lifetime and the photoelectric response [6], but it also leads to higher cost and problem with portability, especially when high repetition rate is required.

Therefore, it is necessary to design a novel PCSS with an electric power switch structure vertically integrated to share the dc-bias voltage. Considering that the repetition rate of a traditional PCSS can reach up to hundreds of megahertz, the structure of multi-cell U-shape n-channel MISFET is the best selection to the design of the novel PCSS. In this letter, the design principles are presented, the voltage and the current formulas are deduced, and the expected effect is validated through the simulation of a relevant GaN-based device sample.

Manuscript received February 18, 2015; revised March 13, 2015; accepted March 14, 2015. Date of publication March 24, 2015. This work was supported in part by the National Natural Science Foundation of China under Grant 60906029 and in part by the University of Illinois at Chicago, Chicago, IL, USA. The review of this letter was arranged by Editor T. Egawa.

X. Wang is with the Xi'an University of Technology, Xi'an 710048, China. She is now a visiting scholar at the University of Illinois at Chicago, Chicago, IL 60607 USA.

S. K. Mazumder is with the University of Illinois at Chicago, Chicago, IL 60607 USA (e-mail: mazumder@uic.edu).

W. Shi is with the Xi'an University of Technology, Xi'an 710048, China.

Color versions of one or more of the figures in this letter are available online at http://ieeexplore.ieee.org.

Digital Object Identifier 10.1109/LED.2015.2416188

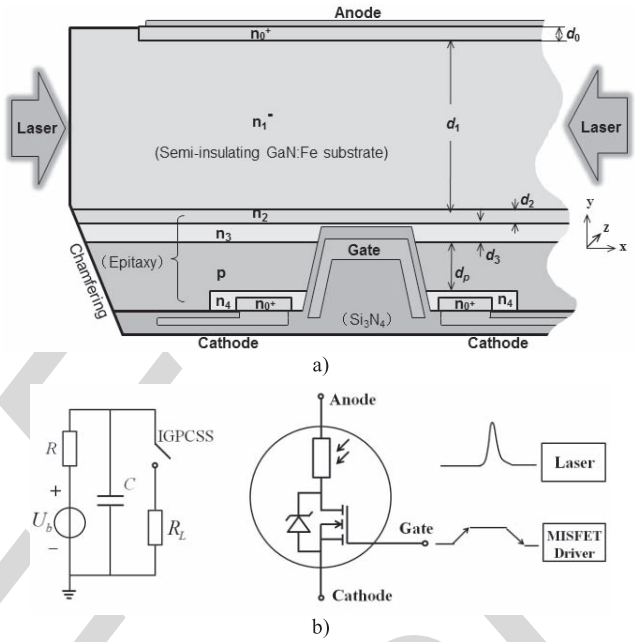

Fig. 1. a) Lateral view of the GaN-based IGPCSS. b) Equivalent circuit model of the IGPCSS device (middle), illustrating the schematic diagrams of a bias source (left) and the timing sequence of trigger signals (right).

II. Design

A. IGPCSS Structure and Triggering Method

The insulated-gate PCSS structure is illustrated in Figs. 1a and 2. The U-shaped MISFET cells are fabricated in the GaN epitaxy layers which grow on a semi-insulating GaN:Fe substrate. The unintentionally-introduced shallow donor levels in the GaN substrate result from the O on N-sites, Si on Ga-sites and N-vacancies [7], [8]. The iron impurities, as deep acceptor sources, are intentionally heavy doped ($\sim 10^{18}$ cm^{-3}) to compensate the shallow donors for making the substrate dark resistivity up to $1 \times 10^9 \Omega \cdot$cm, and meanwhile the substrate carrier lifetime sharply decreases to $<$ 1ns [3]. A gate-voltage pulse makes the channel entirely open and then two rows of 1-ns-pulsewidth 1-mJ-energy 532-nm-wavelength laser beams simultaneously illuminate the semi-insulating substrate from opposing sides. The equivalent circuit model composes of a traditional PCSS, an n-channel normally-closed MISFET, and a voltage-stabilizing diode, as illustrated in Fig. 1b.

A few of methods are used to increase the safe operating area of the IGPCSS. The laser fibers are grouped into two rows, and the directions of the laser beams are interdigitated each other (see Fig. 2) to prevent the current crowding happened in the laser-triggered area. The multi-cell parallel connection and the light-doping transition (see n_3 and

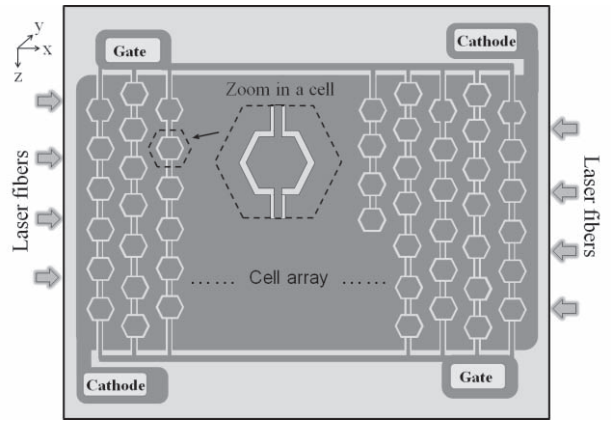

Fig. 2. Bottom view (upper half) of the GaN-based IGPCSS.

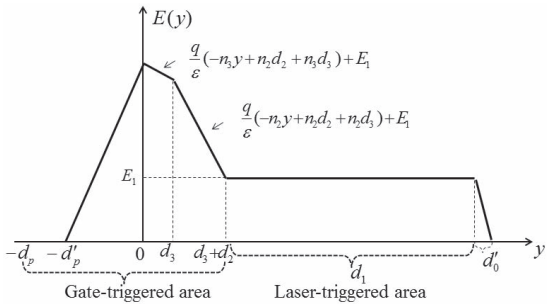

Fig. 3. Electric-field distribution of the IGPCSS under dark-state condition and a dc-bias voltage.

n_4 layers) for the n-channels terminals are designed to prevent the current crowding enhenced in the gate-triggered area. Furthermore, the chamfer processes is helpful to improve the blocking voltage ability of the gate-triggered area.

B. Static Voltage Distribution

The static distribution of the electric field across the IGPCSS before it is triggered by an electrical gate signal is shown in Fig. 3. The space charges in the n_1 layer can be ignored due to the semi-insulating property, and hence the electric field across the n_1 layer in the y direction (E_1) is regarded as a constant. The voltage drop due to the bulk resistances of the n_4, p, n_0 layers can be ignored, since their conductivities are much higher than that of the semi-insulating substrate. Moreover, the voltage drop across the positively biased p-n_4 junction can be ignored when the IGPCSS is biased with high voltage. Therefore, through integrating the electric field curve of Fig. 3, the static voltage across the gate-triggered area is given by

$$V_{th} = k\left[\frac{q}{\varepsilon}\left(\frac{pd_p'^2}{2}+\frac{n_3d_3^2}{2}+n_2d_2d_3+\frac{n_2d_2^2}{2}\right)+E_1\,(d_2+d_3)\right],$$
$$E_1=\frac{U_b-V_{th}}{d_1},\quad d_p'=\frac{n_2d_2+n_3d_3+\frac{\varepsilon E_1}{q}}{p}. \quad (1)$$

In (1), q is the elementary charge, ε is the dielectric constant of the epitaxial material, and k (<1) is a semi-empirical coefficient which is used to linearly simplify the effect caused by the x-directed extension of the carrier-depleted region along the insulated gate. It is noted that, the thickness of the p-type epitaxy layer (d_p in the Fig. 1) should be more than the minimum design value (d_p'), or the pn junction will be punched through undesirably from the cathode side. Equation (1) yields that V_{th} will monotonically slightly change following the bias voltage and the substrate thickness, as shown in Fig. 4.

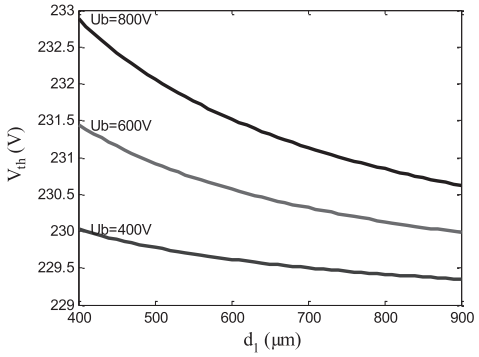

Fig. 4. Variation of the static voltage across the gate-triggered area of the IGPCSS under dark-state condition for varying the dc-bias voltages (U_b) and the substrate thickness (d_1). The curves are calculated based on (1) where $d_2 = 1.5$ μm, $d_3 = 0.5$ μm, $k = 0.25$ and n_2, n_3 and p are 5×10^{16}, 1×10^{15}, and 8×10^{15} cm^{-3}, respectively.

C. Photocurrent Distribution

To design the relevant heat-dissipation accessory of the IGPCSS, the photocurrent distribution in the x direction is estimated roughly. The density of the gallium-site Fe^{3+} deep energy level is much higher than those of any other energy levels in the GaN:Fe [8]. It means that the two-step photon absorption from valence band to conduction band via the Fe^{3+} levels is dominant, if the laser wavelength is less than 585 nm (i.e., 3.42 eV-1.299 eV [8]). Therefore, the optical intensity distribution in the IGPCSS can be given by

$$I(x,t)=I_0[e^{-\alpha_{eff}x}+e^{-\alpha_{eff}(L-x)}]G(t). \quad (2)$$

In (2), I_0 is the initial optical intensity of the incident laser only from one side of the IGPCSS, G is a Gaussian function, and α_{eff} is the effective absorption coefficient to linearly simplify the two-step photon absorption via the high-density deep energy levels [3]. Considering that the cost of the power pulsed laser device is typically incorporated in the total cost of the switch system, the lost laser energy transmitted from the opposite sides of the IGPCSS is expected to be less than 5% of the incident energy. The x-directed device length (L) can be roughly estimated based on (2).

The rate for the photon-generated electrons (n) in the semi-insulating GaN substrate is given by

$$\frac{\partial n(x,t)}{\partial t}=-\frac{1}{2\hbar\omega}\frac{\partial I(x,t)}{\partial x}-\frac{n(x,t)}{\tau_r} \quad (3)$$

where $\hbar\omega$ is the photon energy and τ_r is the effective recombination rate. Therefore, the peak electron density is deduced by setting $\frac{\partial n(x,t)}{\partial t}=0$ to obtain the following:

$$n\left(x,t_{peak}\right)=\frac{\tau_r\alpha_{eff}}{2\hbar\omega}I\left(x,t_{peak}\right) \quad (4)$$

where $I\left(x,t_{peak}\right)$ is obtained using (2). The peak conductivity is given by

$$\sigma(x,t_{peak})=qn(x,t_{peak})(\mu_n+\mu_p) \quad (5)$$

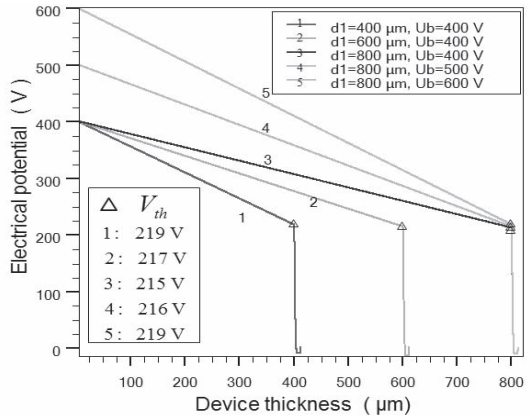

Fig. 5. Static voltage distribution in the y direction, simulated when $d_0 = 0.5\ \mu$m, $d_2 = 1.5\ \mu$m, $d_3 = 0.5\ \mu$m, $d_p = 10\ \mu$m, and n_0, n_1, n_2, n_3, n_4 and p are 8×10^{19}, 6.2×10^6, 5×10^{16}, 1×10^{15}, 1×10^{17} and 8×10^{15} cm^{-3}, respectively.

where μ_n and μ_p are the electron and the hole mobilities, respectively. The current density is proportional to the conductivity, which results in

$$J\left(x, t_{peak}\right) \propto [e^{-\alpha_{eff}x} + e^{-\alpha_{eff}(L-x)}]. \quad (6)$$

III. Analysis and Comparison

The static voltage distributions are simulated using Silvaco [9] and the results are shown in Fig. 5. The voltage across the gate-triggered area slightly decreases with d_1 and slightly increases with U_b. These variations are in agreement with the above conclusions calculated based on (1). It is noted that, the voltage across the gate-triggered area is approximatively a constant, which validates the equivalent circuit model of the IGPCSS in Fig. 1b. Therefore, there exist two thresholds for the IGPCSS device to output photocurrents: one, which represents the gate voltage when the n-channels are just formed; and the other, which represents the bias voltage when the p-n junction is just punched through.

Next, the leakage current and the transient characteristics of an IGPCSS with a punch-through voltage of 400 V are simulated. The simulation model and the results are shown in Fig. 6. With the IGPCSS being electrically triggered by the gate, the voltage across the gate-triggered area is gradually transferred to the laser-triggered area (see the orange curve in Fig. 6c), which enhances the electric field across the IGPCSS laser-triggered area from 6.7 kV/cm to 13.4 kV/cm.

Third, a comparable traditional PCSS (CT-PCSS) model (see Fig. 6b) are simulated, which have the same material, size, ohmic electrodes, static electric field and laser as that of the IGPCSS. The result demonstrates that the leakage current of the IGPCSS is far less than that of the CT-PCSS owing to the p-n junction. Furthermore, the results demonstrate that the IGPCSS yields higher photocurrent peaks than the CT-PCSS. The photoelectric-conversion efficiency of the IGPCSS (η_{IG}) is higher than that of the CT-PCSS (η_{CT}). The photoelectric-conversion efficiency is referred in this letter as the ratio of the output photocurrent peak and the relevant input single-pulse laser energy. The efficiency increment ($\eta_{\mathrm{IG}} - \eta_{\mathrm{CT}}$) is approximatively proportional to $U_b/(U_b - V_{th})$ if the enhenced transient electric field across the IGPCSS laser-triggered area is still in the velocity-field linear range (i.e., below 200 kV/cm for the wurtzite GaN material used [10]. Considering V_{th} is almost a constant for varying U_b, it is concluded that, the photoelectric-conversion efficiency of the IGPCSS can be controlled relatively easily by varying the dc-bias voltage.

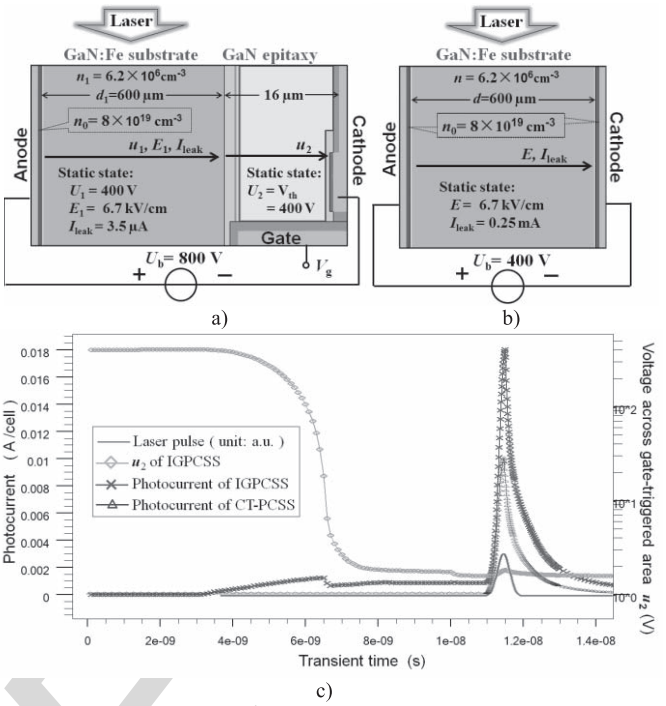

Fig. 6. Characteristics of a) the IGPCSS and b) the CT-PCSS. c) Transient simulation results for the IGPCSS when the gate voltage of the IGPCSS linealy rises from 0 V to 10 V in the first 10 ns and then stays at 10V.

IV. Conclusion

A novel insulated-gate photoconductive semiconductor switch (IGPCSS) structure is presented. It attains a monolithic integration of a PCSS and MISFET cells thereby yielding less leakage current and higher photoelectric-conversion efficiency compared to a relevant traditional PCSS. Through the simulation analyses of the static and the dynamic characteristics, the GaN-based IGPCSS design is validated.

References

[1] P. Kirawanich, S. J. Yakura, and N. E. Islam, "Study of high-power wideband terahertz-pulse generation using integrated high-speed photoconductive semiconductor switches," *IEEE Trans. Plasma Sci.*, vol. 37, no. 1, pp. 219–228, Jan. 2009.

[2] W. Shi and Z. Fu, "2-kV and 1.5-kA semi-insulating GaAs photoconductive semiconductor switch," *IEEE Trans. Electron Device Lett.*, vol. 34, no. 1, pp. 93–95, Jan. 2013.

[3] J. H. Leach *et al.*, "High voltage bulk GaN-based photoconductive switches for pulsed power applications," *Proc. SPIE, Gallium Nitride Mater. Devices VIII*, vol. 8625, pp. 86251Z-1–86251Z-7, Mar. 2013.

[4] J. S. Sullivan and J. R. Stanley, "6H-SiC photoconductive switches triggered at below bandgap wavelengths," *IEEE Trans. Dielectr. Electr. Insul.*, vol. 14, no. 4, pp. 980–985, Aug. 2007.

[5] J.-H. Kim *et al.*, "High voltage Marx generator implementation using IGBT stacks," *IEEE Trans. Dielectr. Electr. Insul.*, vol. 14, no. 4, pp. 931–936, Aug. 2007.

[6] S. F. Glover *et al.*, "Pulsed- and DC-charged PCSS-based trigger generators," *IEEE Trans. Plasma Sci.*, vol. 38, no. 10, pp. 2701–2707, Oct. 2010.

[7] D. O. Dumcenco *et al.*, "Characterization of freestanding semi-insulating Fe-doped GaN by photoluminescence and electromodulation spectroscopy," *J. Appl. Phys.*, vol. 109, no. 12, pp. 123508-1–123508-6, Jun. 2011.

[8] A. Y. Polyakov *et al.*, "Properties of Fe-doped, thick, freestanding GaN crystals grown by hydride vapor phase epitaxy," *J. Vac. Sci. Technol. B*, vol. 25, no. 3, pp. 686–690, 2007.

[9] *Atlas User's Manual*. [Online]. Available: http://www.silvaco.com

[10] S. Chen and G. Wang, "High-field properties of carrier transport in bulk wurtzite GaN: A Monte Carlo perspective," *J. Appl. Phys.*, vol. 103, no. 2, pp. 023703-1–023703-6, Jan. 2008.